Canadian Science Publishing
NRC Research Press journals | Publishing Services

Canadian Journal of Chemistry
Revue canadienne de chimie

Prediction of Rate Constants of Important Chemical Reactions in Water Radiation Chemistry in Sub- and Supercritical Water – Non-Equilibrium Reactions

Journal:	*Canadian Journal of Chemistry*
Manuscript ID	cjc-2017-0315.R2
Manuscript Type:	Article
Date Submitted by the Author:	23-Dec-2017
Complete List of Authors:	Liu, Guangdong; Mount Allison University, Physics Landry, Cody; Mount Allison University Department of Chemistry and Biochemistry Ghandi, Khashayar; Mount Allison University, Physics; Mount Allison University Department of Chemistry and Biochemistry
Is the invited manuscript for consideration in a Special Issue?:	SFU
Keyword:	radiation chemistry, supercritical water, kinetics, Generation IV reactors

Prediction of Rate Constants of Important Chemical Reactions in Water Radiation Chemistry in Sub- and Supercritical Water – Non-Equilibrium Reactions

Guangdong Liu[a], Cody Landry[b], Khashayar Ghandi[a,b]*

[a]Department of Physics, Mount Allison University, Sackville, NB E4L 1E2, Canada
[b]Department of Chemistry and Biochemistry, Mount Allison University, Sackville, NB E4L 1E2, Canada

*Corresponding author: Khashayar Ghandi, kghandi@mta.ca, kghandi@triumf.ca

Abstract: The rate constants for reactions involved in the radiolysis of water under relevant thermodynamic conditions in supercritical water-cooled reactors are estimated for inputs in simulations of the radiation chemistry in Generation IV nuclear reactors. We have discussed the mechanism of each chemical reaction with a focus on non-equilibrium reactions. We found most of the reactions are activation-controlled above the critical point and that the rate constants are not significantly pressure-dependent below 300°C. This work will aid industry with developing chemical control strategies to suppress the concentration of eroding species.

Keywords: Generation IV reactors, supercritical water, kinetics, radiation chemistry

1. Introduction

A supercritical water cooled reactor (SCWR) uses supercritical water (SCW) (water above its critical point of 374°C, 221 bar) as its coolant.[1] SCWR is one of the proposed Generation IV reactors by the 2002 Nuclear Energy Research Advisory Committee.[2] SCWRs have advantages, such as increased sustainability, improved safety, and proliferation-resistance.[3] However, the radiolysis (R1) in SCW, which could lead to corrosion, is largely unknown:

$$\text{R1: } H_2O \xrightarrow{\text{ionizing radiation}} e^-_{aq}, H\cdot, \cdot OH, H_2, H_2O_2, HO_2, O_2^-.$$

Chemical control strategies are used to mitigate corrosion in nuclear reactors.[4] In existing nuclear reactors, chemicals such as hydrogen are added to the coolant to chemically react with and suppress the concentration of oxidizing species.[4] In SCWRs, the type of chemicals to add, and the amount to add, if any, are unknown, and are hard to determine experimentally. Computer simulations such as Monte Carlo simulations,[5,6] can be used to find the optimum coolant composition that minimizes the production of corrosive radiolysis products.[7]

In 2009, Atomic Energy of Canada Limited (AECL) published a review of the rate constants for radiolysis of water at temperatures below SCWR conditions.[8] Although the rate constants of reactions in water mostly follow Arrhenius temperature dependence at low temperatures, several studies have shown that the rate constants of many reactions in water plateau and may even decrease near the critical point.[9–16] Accurate predictions of rate constants of relevant reactions in SCW are crucial for the development of chemical control strategies to minimize corrosion in SCWRs.[7,17] The goal of this work is to give recommendations for the rate constants of important reactions in radiolysis of water under hydrothermal conditions based on a model proposed by Ghandi *et al.*[11] that accounts for the non-Arrhenius temperature dependence of different reactions in water. Table S1 in the Supporting Information (SI) contains all reactions. The labeling of reactions are adapted from AECL report.[8] We have previously addressed all the significant equilibrium reactions involved in the radiation chemistry of water (Reactions R23-R32) under SCWRs coolant's thermodynamic conditions.[7] This paper addressed the non-equilibrium reactions (Reactions R2-R22a) which are grouped according to their mechanisms in Table 1. The methodology was described in detail previously[13] and in the SI.[7]

Although all reactions that are discussed in this paper (R2-R22a) are important in the radiolysis of water, in order to make the main text of this paper as concise as possible we had to transfer discussion of many reactions to the SI. The splitting of the reactions that are discussed in the main text vs. those in SI is mainly done based on g-values. The g-value is defined as the number of species formed or dissociated per 100 eV energy absorbed. Some species in water such as ·OH, e_{aq}^-, H· and H_2 have larger g-values at around 350°C,[8] and are expected to be important in SCW as discussed in section 2.6. Thus, their reactions should be given more attention as they can significantly change the outcome of Monte Carlo simulations.[7] As such, we discussed these reactions (R3, R4, R5, R6, R7), and the reactions that require special

treatments to model in the main text (R2, R15), while discussion of the other reactions are provided in the SI. Despite this splitting of reactions, we strongly recommend that the readers also carefully study all reactions we discussed in the SI. The readers who model the radiation chemistry in coolants of SCWR should know that the tables of all reaction rate constants and activation parameters are reported in the SI. A brief summary of all reactions involved (including the equilibrium reactions) is provided at the end of the main text. Since we both describe and classify the reactions based on their mechanisms, the reactions are not discussed in numerical order (e.g. R4 is discussed before R3 and R2, etc.)

2. Results and Discussion

2.1 The cage effect

A model that considers the number of collisions during the lifetime of an encounter pair is used in this work to account for the observed significant decrease of rate constants of reactions in water at high temperatures.[7,11] The process in which reactant species diffuse together to become neighbors is called an encounter. In order for a reaction to occur, diffusion of the reactants into the same water cage is required. The solvent cage will keep the reactants in close proximity for a while, during which they will collide with each other and with the water molecules surrounding them. The lifetime of an encounter is the time that the reactants remain within the same water cage. The temperature dependence of the encounter time at a certain pressure is discussed when introducing the first reaction we investigated.

For a reaction to occur, the reactants must be oriented properly to allow new bonds to form. Once the reactants enter the same water cage, they will collide with each other, reorient, and exchange energy with surrounding molecules until they are either properly oriented for the

reaction to occur, or they will escape from the cage. When temperature increases, the hydrogen bond (H bond) length also increases and thus H bond becomes weaker.[18] As a result, the energy barrier to escape a cage formed by these bonds decreases. This has two implications, the first being reactants moving from cage to cage faster (larger diffusion coefficients) and the second being that reactants, once in the same cage, have a shorter encounter lifetime to accommodate proper orientation for reaction. As a result, the probability that the reactants will find the right orientation to react decreases, and therefore the efficiency of the reaction is reduced.[7,11] This is accounted for in our model by including an efficiency factor, f_R, which is proportional to the number of collisions per encounter. This is described further when discussing Reaction R4 and in the SI.

2.2 Addition / Non-dissociative attachment

As will be described in section 2.3, Reaction R2 is heavily influenced by Coulomb interactions. Reaction R3 is only influenced by spin orientation not the orientation of reactants. On the other hand, in reaction R4 ($\cdot OH + \cdot OH \rightarrow H_2O_2$), the ·OH radicals must approach each other in an orientation that allows new bonds to be formed between the O atoms, hence influenced by the cage effect more than H· atom reactions. Thence we introduced this reaction first, and used it as an example to show the timescales and collisions per encounter and in general the cage effect.

R4:

$$\cdot OH + \cdot OH \rightarrow H_2O_2$$

The self-recombination of hydroxyl radicals produces hydrogen peroxide, which can decompose into molecular oxygen and water. This reaction is important in SCWRs, as the crack growth rate in reactors is related to H_2O_2 and O_2.[19] The reaction has been studied by Jannik *et*

106 *al.*[20] from 150 to 350°C at 250 bar, by directly measuring ·OH radical transient optical absorption
107 at 250 nm. They suggested the use of the Noyes equation to describe the non-Arrhenius
108 behavior. In their system, hydrogen radicals reached up to 30% of the total yield of hydroxyl
109 radicals at 350°C. Due to the ambiguity of the extinction coefficient at higher temperatures, the
110 actual rate will differ from the measured one in the high-temperature range.[20] Elliot *et al.*[21]
111 studied the same reaction from 20 to 200°C. Both studies are done using N_2O saturated solution
112 because solvated electrons react with N_2O and convert them to ·OH radicals.

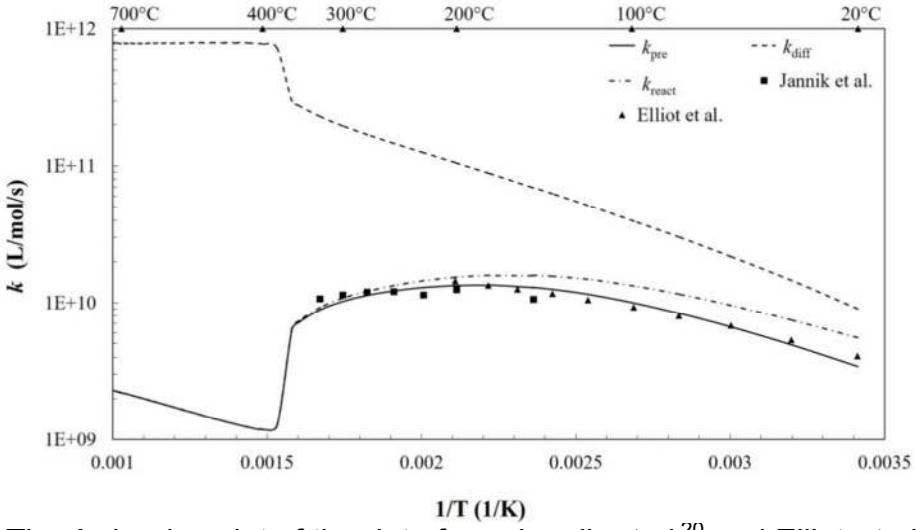

113 Figure 1 The Arrhenius plot of the data from Jannik *et al.*[20] and Elliot *et al.*[21], with our fit of k_{pre}
114 to the data and extrapolations to high temperatures for R4: ·OH + ·OH → H_2O_2 at 250 bar.

115 Elliot found an activation energy of 3.7 kJ mol^{-1} which is smaller than our fit value 12 kJ mol^{-1}.
116 This reaction is not a diffusion-controlled reaction, as can be seen from our fits. It is strongly
117 influenced by the cage effect as can be seen by the rapid drop in reaction rate near the critical
118 point in Figure 1. This is the reason for the difference in our activation energy and the one
119 reported by Elliot *et al.*[21] Figure 1 suggests that although there are enough encounters for the
120 reaction, the efficiency of the reaction at high temperatures is low due to the cage effect (the
121 ·OH radicals are not able to find the right orientation to react before leaving the water cage).

Therefore, the f_R factor will be a small number at high temperatures. To estimate the duration of encounter τ_{enc}, we assumed the encounter pairs are in equilibrium with the separated reactants. The equilibrium constant can be written as the ratio of the diffusion rate constant and the separation rate of the reactants: $K_{enc} = k_{diff}/\tau_{enc}^{-1}$.[11] K_{enc} can be estimated by considering the probability of finding one reactant as next nearest neighbor to the other. Using a coordination number of 8, we found $K_{enc} = 8 / [H_2O]$. Then, τ_{enc} can be calculated using the formula:[11]

$$\tau_{enc} = \frac{8}{k_{\mathrm{diff}} \times [H_2O]}. \qquad [1]$$

The duration of collision τ_{coll} can be estimated based on collision time in gas-phase, collision frequency, scaled with the inverse self-diffusion constant of the solvent:[11]

$$\tau_{coll} = Z^{-1}(\rho) = Z_0^{-1} D(\rho)/D(\rho_0) \qquad [2]$$

where ρ is density, Z_0^{-1} is scaling constant, $D(\rho)$ is self-diffusion constant of water at a given temperature, and $D(\rho_0)$ is self-diffusion of water at reference state which is chosen to be 450°C and 240 bar consistent with previous work.[11] The τ_{coll} / τ_{enc} gives the number of collisions per encounter (Figure 2). There are around 1000 collisions per encounter for this reaction at lowest temperature. Other reactions have an order of 10^2 to 10^3 collisions per encounter at room temperature. In SCW, the weak H bonds do not hold water molecules together for more than 1 ps as opposed ~31 ps at room temperature,[18,22] and the number of H bonds per water molecule decreases as temperature is increased at a given pressure.[23] As temperature increases to near the critical point, collisions per encounter decrease and the value of f_R also decreases.[7]

The temperature dependence of f_R and collisions per encounter are similar (Figure 2). At room temperature f_R is around 1 and as temperature increase to near the critical point, it decreases to about 0.001 to 0.01.[7] Above the critical point, at high enough temperatures there is one collision per encounter, thus f_R remains constant.

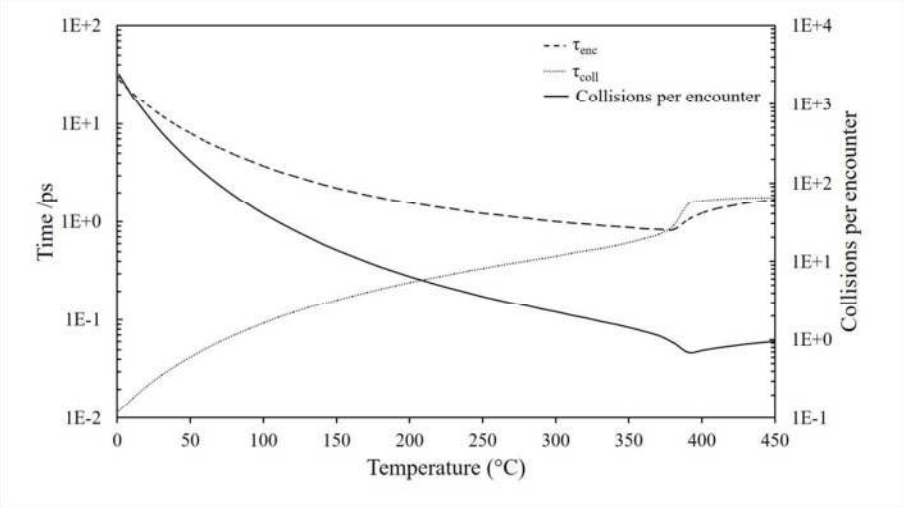

Figure 2 τ_{enc} and τ_{coll} (y-axis on the left), and collisions per encounter (τ_{coll}/τ_{enc}, y-axis on the right) for R4.

Including f_R in Arrhenius equation, the temperature dependence will be like Figure 1. It goes through a maximum before the critical point, before increasing via an Arrhenius temperature dependence. The rate constants of most reactions studied in this work follow a similar temperature dependence thus their details are only reported in the SI.

R3:

$$H\cdot + H\cdot \rightarrow H_2$$

The recombination of H· atoms between 20 and 250°C at 140 bar was measured by Sehested *et al.*,[24], by observing the UV spectrum of the H· atom at pH 2. Their rate constants are lower limits of the real values at higher temperatures because the extinction coefficient was assumed

to be temperature independent, but it increases by 10% from 20 to 200°C.[24] They obtained an activation energy of 14.7 kJ mol^{-1}; the activation energy from our fit is 7.8 kJ mol^{-1}.

Sehested and Christensen did not account for the spin exchange [11]. The addition reaction, however, is in competition with the spin exchange. Electron spin exchange is common in low energy collisions between species with unpaired electron.[25] For example, a collision between two H· atoms of spin states $|\alpha_p\alpha_e\rangle$ and $|\beta_p\beta_e\rangle$ (α is spin up, β is spin down, p denotes the proton, and e denotes the electron), will result in $|\alpha_p\beta_e\rangle$ and $|\beta_p\alpha_e\rangle$, if spin exchange occurs. Similar to the collisions per encounter of hydroxyl radicals in Figure 2, there are more collisions during an encounter of two hydrogen atoms of opposite electron spins at low temperatures (the reaction happens only if the electron spins are opposite). At each collision, a spin exchange or an addition reaction can occur. Although spin exchange will not prevent an addition reaction, an addition reaction will prevent a spin exchange. If there are more collisions in an encounter, an addition reaction will eventually occur. Thus, it is reasonable to assume this reaction is diffusion-controlled at low temperatures. At high temperatures, there is essentially only one collision during an encounter. Therefore, the probability of the H· atoms going through an addition reaction is significantly smaller at higher temperatures.

For spin exchange, the rate constant depends on the number of encounters, $k_{diff;}$ the exchange factor, p_{spin}, and the strength of the exchange interaction, J [11]:

$$k_{\mathrm{pre}} = p_{\mathrm{spin}} k_{\mathrm{diff}} f_{\mathrm{J}}; \quad f_{\mathrm{J}} = J^2\tau_{\mathrm{enc}}^2/(1 + J^2\tau_{\mathrm{enc}}^2) \qquad [3]$$

where τ_{enc} is the duration of the encounter, k_{diff} is the diffusion rate constant. For a strong spin exchange limit, k_{pre} only depends on p_{spin}. For weak a spin exchange, f_J shows a similar

temperature dependent trend as f_R factor, although instead of orientation, f_J only depends on the number of collisions in an encounter.[11]

For this reaction, orientation is not an important factor considering the electronic aspects; only the spin orientation is important. Also since H-atom reactions could be affected by quantum tunneling at low temperatures, this reaction could be diffusion-controlled in this range. Hence, the possibility of contribution from a diffusion-controlled mechanism at high temperatures cannot be discounted. We have already shown in our previous work that the Stoke-Einstein diffusion model underestimates diffusion coefficients above the critical point.[7] As such, we used a scaled diffusion model of water by Kallikragas *et al.* [26] at high temperatures, and the Stoke-Einstein diffusion model at low temperatures up to 250°C and matched the value of these two curves at 250°C, because at this point we still know the rate constant from the experiment data (Figure 3**)**.

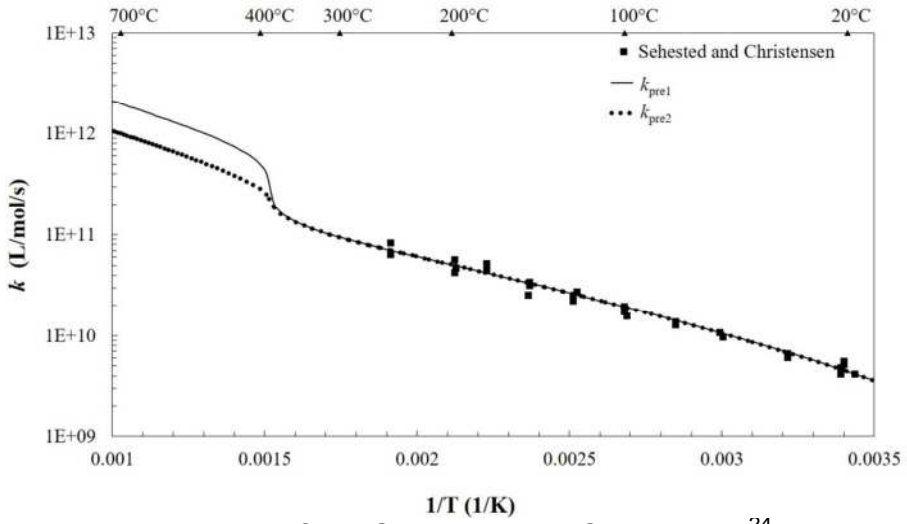

Figure 3 The experimental data from Sehested and Christensen[24], along with our fit of k_{pre1} to the experimental data and its extrapolation to high temperatures for R3. We assumed a diffusion-controlled reaction for R3. For k_{pre2}, we took into consideration the competition with spin exchange as described in the text.

We can correct the rate constants to account for the statistical factor (addition vs. spin exchange) if in each collision the probability of an addition reaction is p_{coll}. We can estimate the number of collisions, n_{coll}, in an encounter at different temperatures using the f_R factor, assuming only one collision per encounter at very high temperature. The probability that an addition reaction occurs in an encounter is calculated as:

$$p_{\mathrm{add}} = 1 - (1 - p_{\mathrm{coll}})^{n_{\mathrm{coll}}} \qquad [4]$$

Multiplying this probability by the diffusion rate constants**,** and assuming p_{coll} is 0.5, we obtain k_{pre2} in Figure 3. The p_{coll} is chosen to be 0.5, but the real value could be slightly smaller. We report the rate constants in the SI for both the diffusion-controlled model, and the diffusion-controlled model in which we accounted for the competition between addition and spin exchange. We recommend the latter.

R6:

$$\mathrm{e_{aq}^-} + \cdot\mathrm{OH} \rightarrow \mathrm{OH^-}$$

The reaction between a hydrated electron and hydroxyl radical is important: it changes the pH of the solution in the radiolysis track and turns ·OH radicals into less reactive OH^- ions. pH is a critical factor for corrosion control in water-cooled nuclear reactors, since it is a significant parameter that affects the speciation and solubility of metal oxide and hydroxides (corrosion passivation layers).[27] A recent Monte Carlo study by Kanike *et al.*[28] shows that a spur formed in the radiolysis of room temperature water is acidic in the early stage, and becomes neutral with time. The increase in pH is mainly due to two reactions: H_3O^+ reacting with OH^-, and H_3O^+ reacting with e_{aq}^-.[28] R6 plays an important role here, as it is linked to the two species. This

211 shows that it is important to have accurate rate constants in order to model water radiolysis
212 since the population of all species are related by different reactions.

213 R6 has been studied by Christensen *et al.*[29], Elliot *et al*. [30], and Janik and Bartels.[8]
214 Christensen *et al.*[29] studied it with pulse radiolysis at a pH of 10.0 to 10.6 using a buffer, and
215 Elliot *et al*. [30] studied this reaction using a deoxygenated borate-buffered solution of pH 9.2. All
216 rate constants were obtained by observing the decay of hydrated electrons in either a buffer or
217 in alkaline water. There is a reasonable agreement between the work of Elliot *et al*.[30] and Janik
218 and Bartels[8], while data from Christenson *et al.*[29] suggests higher rate constants. Our fit shows
219 that R6 is an activation-controlled reaction at high temperatures with a small activation energy of
220 4 kJ mol^{-1}, and a diffusion-controlled reaction up to ~ 200°C (Figure 4). This reaction is a
221 diffusion-controlled reaction at room temperature, and the k_{diff} for this reaction is larger than R3
222 at this temperature. This is likely due to the hydrated electron having a faster diffusion rate than
223 H·, and also the ·OH radical has a larger reaction radius than H·.[21]

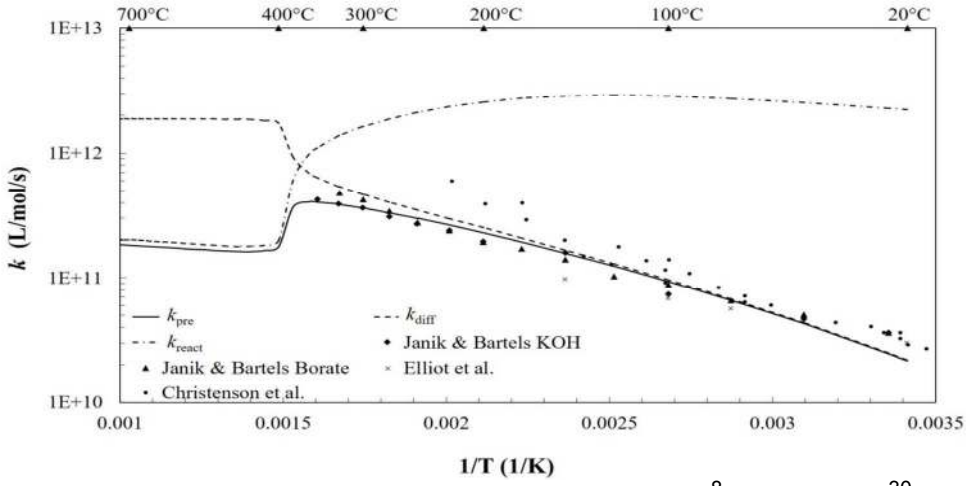

224 Figure 4 The experimental data from Janik and Bartels[8], Elliot *et al.*[30], and Christenson *et al.*[29],
225 along with our fit of k_{pre} to the experimental data and its extrapolation to high temperatures for
226 R6: $e_{aq}^- + \cdot OH \rightarrow OH^-$. A pressure of 250 bar is used in this figure.

R7:

$$H\cdot + \cdot OH \rightarrow H_2O$$

This reaction has been studied by Lundstrom *et al.*[31] and Buxton and Elliot.[32] Lundstrom *et al.*[31] studied this reaction at 100 bar between 5 and 233°C at pH = 2 (Figure 5). They reported an activation energy of 8.2 ± 0.4 kJ/mol,[31] close to our activation energy, 11 kJ mol^{-1}.

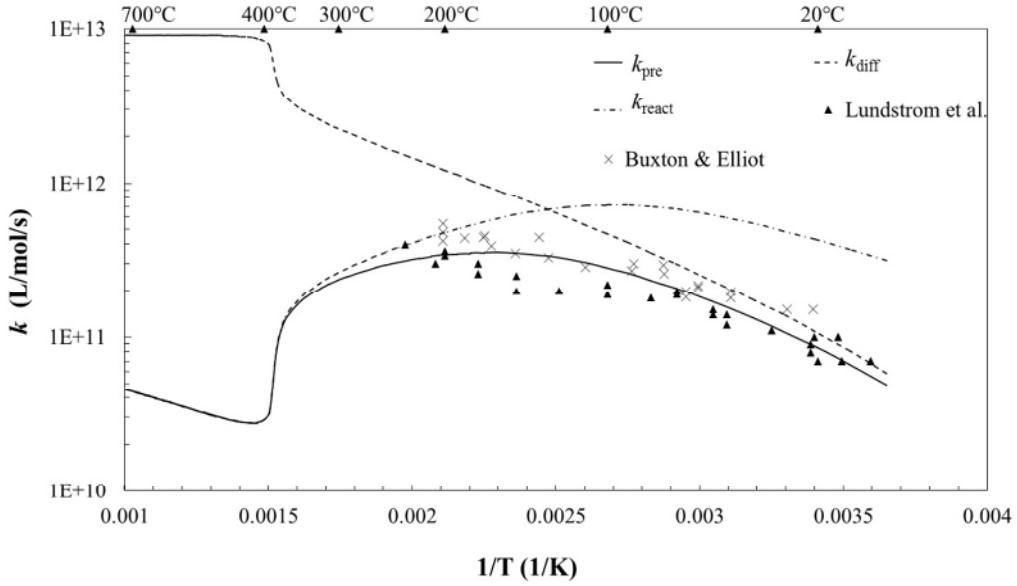

Figure 5 The experimental data from Lundstrom *et al.*[31] and Buxton & Elliot[32], along with our fit of k_{pre} to the experimental data and its extrapolation to high temperatures for the reaction R7: H· + ·OH → H_2O. A pressure of 250 bar was used.

Buxton and Elliot[32] studied R7 up to 200°C using pulse radiolysis of 10^{-2} mol dm^{-3} $HClO_4$ solution. The extinction coefficient was assumed to be independent of temperature in both papers, but it is believed that the extinction coefficient does change with temperature.[8] Buxton compares this reaction with two other reactions (R3 and R4) and finds that R7 is closer to R4 than R3; therefore, they qualitatively conclude it is not a diffusion-controlled reaction. However, our fitting shows a diffusion-controlled reaction at low temperatures up to at least 50°C.

Although the diffusion rate of H· is higher than that of the ·OH radical, the reaction radius of ·OH is larger than the reaction radius of the H· atom at room temperature.[21,33] This is likely the reason that the k_{diff} of R7 and R4 are higher than R3 at low temperatures. Our predictions show a peak rate constant at around 180°C. The rate constant then rapidly drops until about 352°C.

R15:

$$H\cdot + O_2^- \rightarrow HO_2^-$$

Experimental rate constants do not exist for this reaction. Thus, we did quantum calculations for the gas phase at room temperature with Gaussian 09[34] using a density function theory (DFT)[35] with the B3LYP functional[36,37] (UB3LYP) and a basis set of 6-311 ++ G(d,p)[38]. The transition state is calculated using the STQN method.[39] The frequency calculation is performed at the same level to confirm that the structure found in the calculation is a transition state (i.e. with a single imaginary frequency) and to study the thermal effects on activation parameters. From the frequency calculation, the activation entropy ($\Delta S^{\ddagger}$) and enthalpy ($\Delta H^{\ddagger}$) can be obtained. The gas phase activation energy (E_a) and the pre-exponential factor (A) can be calculated using the formula [5] and [6]:[19,40]

$$E_a = \Delta H^{\ddagger} + 2RT \qquad [5]$$

$$log_{10}(A) = log_{10}\left(\frac{e^2 k_B T}{h c_o}\right) + \left(\frac{\Delta S^{\ddagger}}{2.303R}\right) \qquad [6]$$

where R is the gas constant, k_B is the Boltzmann constant, T is the temperature, e is the Euler's number, h is the Planck constant, c_o is the concentration of water. From these calculations, we obtained an activation energy of 42 kJ mol^{-1}, and a pre-exponential factor of 6.0 x 10^{11} dm^3 mol^{-1} s^{-1}. Note that the, computational method using UB3LYP with a basis set of 6-31 + G(d,p) has an

error of around 16 kJ mol^{-1} for activation enthalpy.[41] The basis set we used is likely to yield a more precise result since it uses more functions to describe the valence electrons and has more flexibilities when describing molecular orbitals.[38] It is assumed that the B(r) and $p_R k_{gas}$ (fitting parameters used in this work, described in SI) of R15 are the same as those of R13, as the reactants of R13 are similar to R15, but without charges. The mechanism of this reaction is a hydrogen atom approaching the oxygen pair from an angle of around 55 degrees from the O-O bond. The rate constant of this reaction is shown in

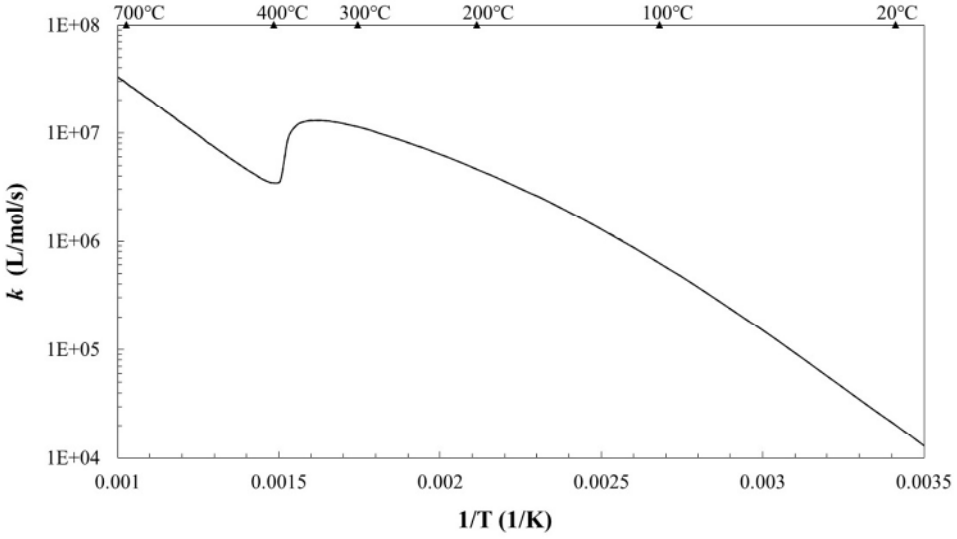

Figure 6. The rate constants for this reaction are small compared to other reactions, thus this reaction should not be significant for modeling radiolysis in supercritical water.

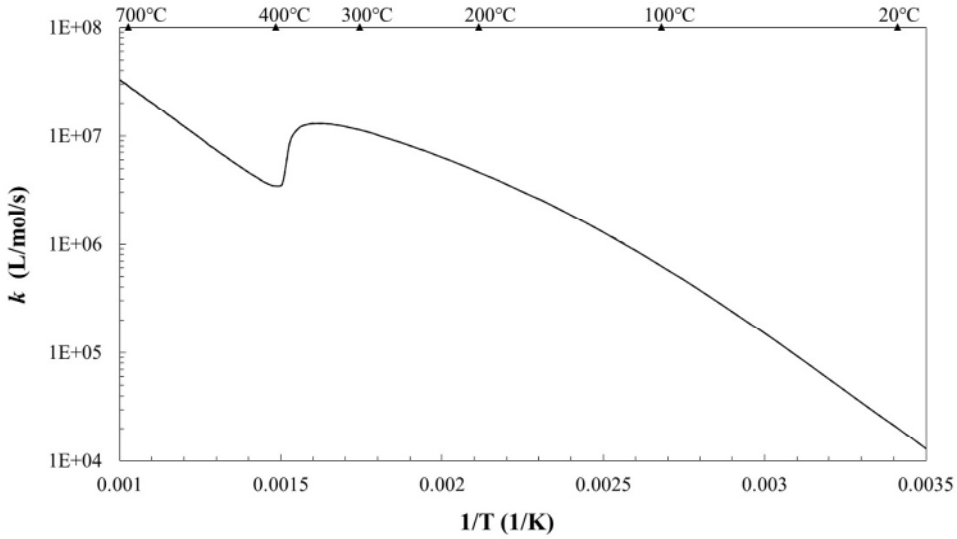

Figure 6 The predicted rate constants of R15: $H\cdot + O_2^- \rightarrow HO_2^-$. The parameters used to obtain this curve are described in the text.

Comparison of different addition / Non-dissociative attachment reactions

Among the addition reactions, R3 is the only one not influenced by the cage effect, since for this reaction, only spin orientation is important, not the orientation of the reactant species. Thus, this reaction is diffusion controlled, hence we used Kallikragas diffusion model. However, the addition reaction is in competition with the spin exchange, thus we also included a statistical factor to account for the spin exchange.

Among the addition reactions in this category, Reaction R4 and R15 are activation controlled reactions in all temperature ranges. Although Reaction R6, R7, R9, R11, R13 and R14 are all diffusion-controlled reactions at low temperatures, Reaction R6, R9 and R11 turn into activation-controlled reactions near the critical point, whereas reaction R7 R13 and R14 turn into activation controlled near 150°C. Different reactions have different shapes of temperature dependency mainly due to the difference in diffusion rate of reaction species, degree of the cage effect on the reactions (that also depends on diffusion constants), as well as the energy barrier and pre-

exponential factor of different reactions. For example, the activation energies for R4 and R7 are about the same, but the pre-exponential factor for R4 is two orders of magnitudes smaller than R7, causing it to be an activation-controlled reaction for the whole temperature range. Reactions R6 and R7 are diffusion controlled at low temperatures, but reaction R7 is influenced heavily by the cage effect, thus it turns into an activation-controlled reaction at a lower temperature than R6. The *E*a and *A* will influence the overall curvature and the magnitude of the rate constants respectively, whereas $p_R k_{gas}$ and $B(r)$ (which influences rate constant k_{diff}) will determine where the peak will be and the magnitude that the rate constants will decrease to near the critical point.

2.3 Hydrogen abstraction reactions

Among H· abstraction reactions, R2 and R10 involve reactants of the same charge. Due to Coulomb repulsion, their rate constants drop significantly at high temperatures when the dielectric constant of water is small. These two reactions are not important for the modeling of SCWRs due to their small rate constants in SCW. R2 is described in the text while R10 is described in the SI. Except R5, the rest of the reactions are discussed in the SI due to the small g-value of reactants.

R2:

$$e_{aq}^- + e_{aq}^- + (2\,H_2O) \rightarrow H_2 + 2\,OH^-$$

The bimolecular decay of hydrated electrons have been the subject of many studies since they were first observed using pulse radiolysis in 1962.[42] Hydrated electrons play important roles in many fields, influencing chemical,[43] biological,[44,45] and radiation processes.[45] Many decades after its discovery, the structural and spectroscopic properties of hydrated electron are still not fully understood.[45–50] Nevertheless, the bimolecular decay of hydrated electrons were

studied by Christensen *et al*.[51] between 5 and 300°C and 140 and 150 bar (Figure 7). This work was done using pulse radiolysis and under high hydrogen pressure, in a high-pressure high-temperature cell with an initial pH ranged from 10.9 to 13, and the final pH ranged from 10.1 to 12.2. In their work, the rate constant showed Arrhenius behavior below 150°C and a diffusion activation energy of 23 kJ mol^{-1} was proposed in that range. The reaction rate dropped rapidly between 150°C and 250°C.[52] Similar behavior has been reported in the work by Marin *et al.*[52] Marin *et al.* studied R2 using pulse radiolysis over the temperature range of 100 to 250°C, with a pressure of 250 bar in alkaline water of pH 10.2 to 11, using increments of 25°C. They reported a maximum rate constant of 5.9 x 10^{10} M^{-1} s^{-1} at 150°C.[52] The rate constants decrease rapidly above 250°C, becoming too small to be reliably measured.[52] Data from both Stuart and Ouellette[53] and Marin *et al.*[52] was used in Figure 7. The data above 250°C is less reliable due to impurities.[52] These studies show the limits of experiments that are based on optical spectroscopy for aqueous systems with high pressure and temperature.

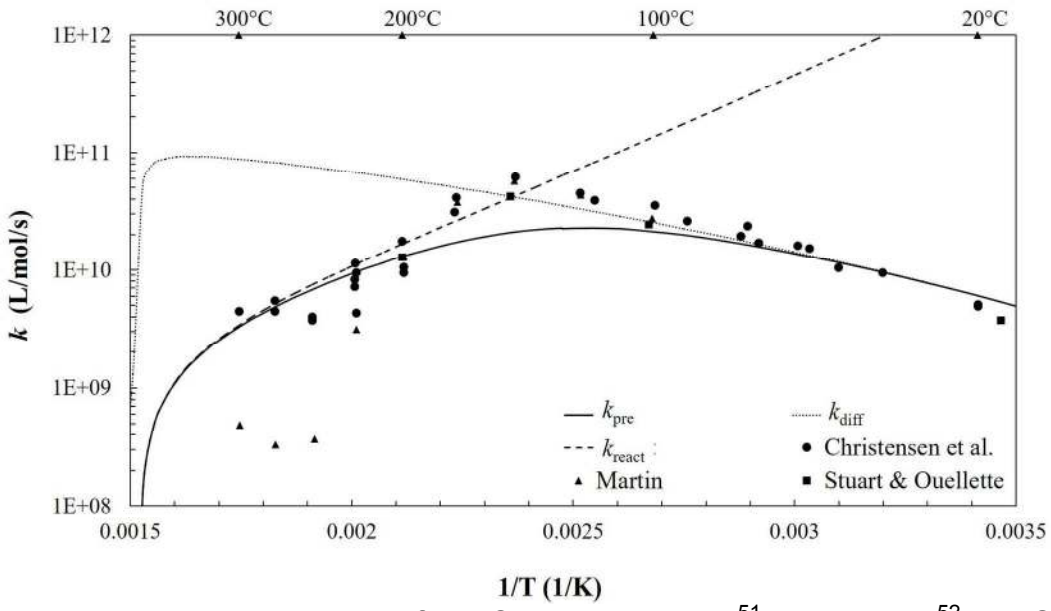

321 Figure 7 The experimental data from Christensen *et al.*[51], Marin *et al.*[52] and Stuart and
322 Ouellette,[53] along with our fit of k_{pre} to the experimental data and its extrapolation to a higher
323 temperatures at 250 bar for R2: $e_{aq}^- + e_{aq}^- + (2H_2O) \rightarrow H_2 + 2OH^-$.

324 Barnett *et al.*[54] studied the double electron evolution reaction $(H_2O)_n^{-2} \rightarrow (H_2O)_{n-2}(OH^-)_2 + H_2$
325 experimentally, using mass spectrometry, and computationally using DFT. In their study, ions
326 mass-to-charge ratio was determined for $(H_2O)_n^{-2}$ water clusters. Only the water clusters that
327 contain more than 105 water molecules have a mass loss of two atomic mass units, indicating a
328 loss of molecular hydrogen. This gives direct evidence of a double electron evolution reaction
329 occurring and shows that this reaction only happens when the water cluster size is larger than
330 105.[54] It also confirms our prediction that this reaction is not important in SCW. Due to the
331 weakening of hydrogen bonding at higher temperatures,[18] there should be a decrease in the
332 number of larger water clusters. If the cluster size had negative temperature dependence, then it
333 would cause the rate constant of R2 to decrease because R2 requires a water cluster size of
334 105 water molecule. A direct attachment of an excess electron on a negatively charged water
335 cluster is inhibited by the large Coulomb barrier and thus, the reaction occurs through the

coalescence of two negative charged water clusters. The two hydrogen atoms from two nearby water molecules in the dielectron hydration cavity approach each other, leading to the formation of a hydrogen molecule.[54] In this step, the calculated energy of the reaction system reaches a maximum,[54] thus this step is the bottleneck of the reaction meaning it follows a hydrogen abstraction mechanism. This is then followed by a two proton transfer from the neighboring donor water molecules to solvated electrons that lead to two hydroxide residues.[54]

On the other hand, Butarbutar *et al.*[55] questioned the validity of applying the sudden decrease of the rate constants in alkaline conditions to neutral conditions. They claimed that such a decrease in the rate constants will result in a discontinuity of their fitted $g(H_2)$ ($g(H_2)$ = 1 meaning a single H_2 molecule is formed when 100 eV radiation is absorbed by the medium) at ~150°C in their low and high linear energy transfer modeling calculations, and that this discontinuity is not observed in experimental data. They suggested a further measurement of rate constants of this reaction in pure water above ~100°C. It has been shown in many works that the reaction of R32r: $H\cdot + H_2O \rightarrow H_2 + \cdot OH$ becomes significantly important at high temperatures.[19,56–58] With this additional channel for H_2 formation, the discontinuity of $g(H_2)$ could be removed though (discussed in detail in section 2.6).

We applied our model to this reaction, which resulted in a fair fit as shown in Figure 7. In Barnett's work, an upper bound for activation barrier of 1.8 eV was proposed based on calculations[54]. This is significantly higher than what we would expect from our fit, or from a diffusion-controlled reaction at room temperature. This is not consistent with the large rate constants observed. The activation energy from other sources, which are obtained from fitting experimental data, are close to the activation energy of self-diffusion of water.[51–53] These predictions similar to ours are significantly lower than the value from Barnett's theoretical study.

As such we believe the proton/electron transfer reaction is significantly affected by quantum tunneling at lower temperatures and that there should be a switch from E_a close to 0 to a large value above the critical point of water, where the large cluster size cannot be accommodated. Furthermore, due to the decrease of the dielectric constant, both the F_D term and $e^{\frac{r_c}{R}}$ term (associated with the Debye factor that account for the change in dielectric constant for reactions of charged species. This is described in detail in the SI) increase by a factor of 5 from room temperature to above the critical point. As a result, the k_{react} and k_{diff} decreased significantly as shown in Figure 7. We expect the rate constants of this reaction to drop dramatically at high temperatures. We do not consider this reaction significant in SCW.

R5:

$$e^-_{aq} + H\cdot(+H_2O) \rightarrow H_2 + OH^-$$

The reaction of a hydrated electron with an H· atom produces H_2 and OH^-. The products of this reaction are similar to those of R2, but this reaction only involves a single hydrated electron. This reaction has been studied in three laboratories.[29,52,59] These studies are based on the hydrated electron extinction coefficient 18400 L mol^{-1} cm^{-1} at maximum absorbance wavelength, which was corrected to 22700 L mol^{-1} cm^{-1} by the work of Elliot and Ouellette.[60]

One of the proposed mechanism of R5 is shown in Figure 8. In this proposed mechanism, orientation should be an important factor. Orientation sensitive reactions are influenced by the cage effect, and the rate constants drop near the critical point. Tunneling can be a factor for this reaction as well, but that is more important at a lower temperature range. The work from Janik and Bartels also indicates that the rate constant of R5 from Marin is too high above 250°C.[8] The

379 significant increase of Marin's data above 250°C could be due to systematic error (eg. high
380 concentration of impurity due to corrosion at high temperature), thus is omitted in our fit.

R5: $e_{aq}^- + H^{\bullet}(+H_2O) \longrightarrow H_2 + OH^-$

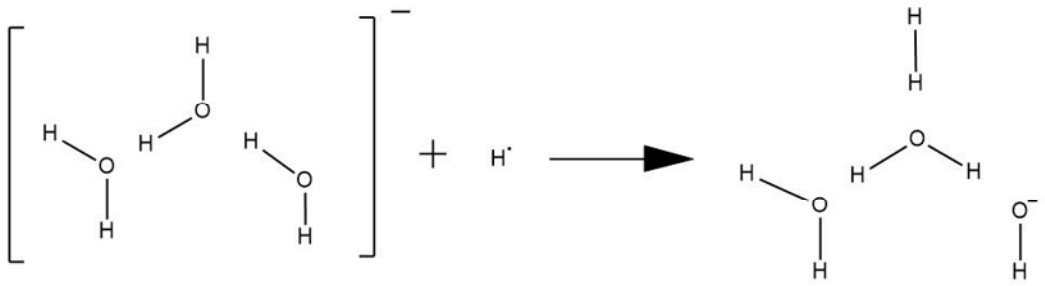

381

382 Figure 8 proposed mechanism for R5. H· atom has to come to close to the O-H bond on the
383 top transfer an H· to form H_2, followed by a proton transfer from a nearby water.

384 Christensen *et al.*[29] extracted the data by fitting the decay of hydrated electron absorption in
385 water containing dissolved hydrogen, which turns hydroxyl radicals into hydrogen atoms in near
386 neutral pH solution in the pressure range of 90 to 140 bar. Schwarz[59] studied R5 in the
387 temperature range of 4 to 65°C and used pulse radiolysis to find a rate constant of 3.4×10^{10}
388 L/mol/s and an activation energy of 16.1 kJ mol^{-1} at 25°C. This data was collected in hydrogen-
389 saturated solutions buffered between pH 8.0 and 8.35 with mixtures of boric acid and sodium
390 tetraborate.[59] We obtained an activation energy of 5.0 kJ mol^{-1} for this reaction.

The rate constant of R5 slowly reaches a peak around 300°C and decreases slowly until it reaches the region near the critical point, where it then rapidly decreases and follows Arrhenius behavior thereafter. This reaction is a diffusion-controlled reaction at low temperatures, but it changes to an activation-controlled as shown in Figure 9. Compared to R3, which is the recombination of H· atoms, in R5 a hydrated electron is reacting with an H· atom. The observed rate constant for R5 is one order of magnitude higher than R3, and they are both diffusion-controlled below 300°C.

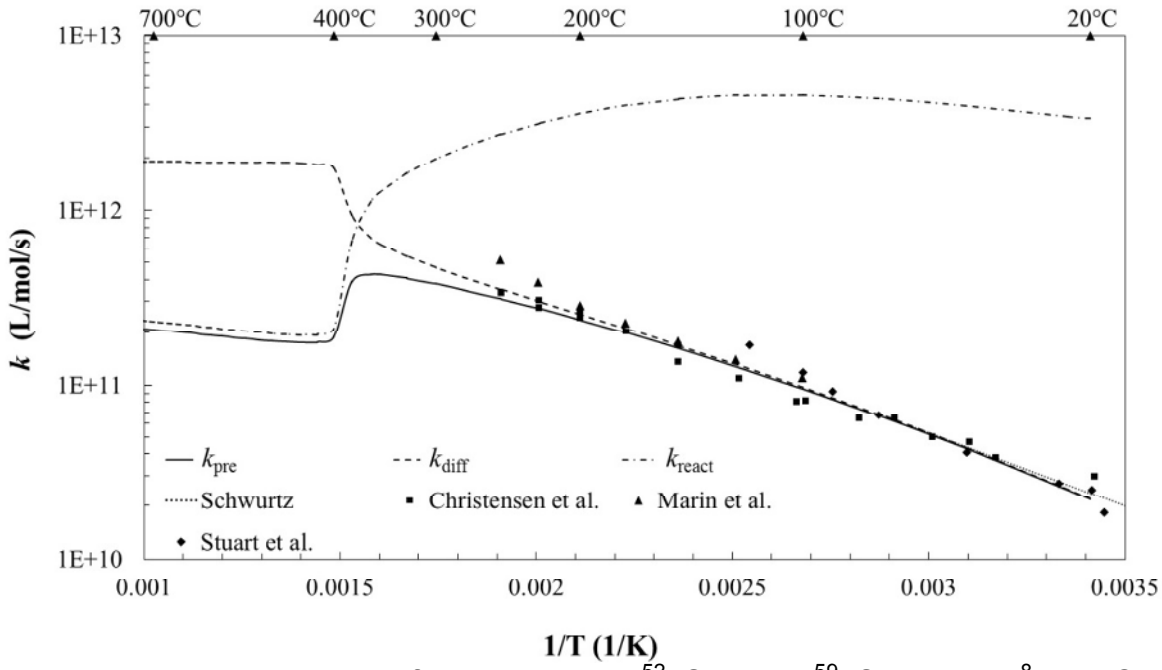

Figure 9 The experimental data from Marin *et al.*[52], Schwurtz[59], Stuart *et al.*[8], and Christensen *et al.*[29], along with our fit of k_{pre} to the experimental data and extrapolation to high temperatures for R5: $e_{aq}^- + H\cdot\ (+ H_2O) \rightarrow H_2 + OH^-$. A pressure of 250 bar was used to produce the figure.

Although diffusion coefficients of H· and e_{aq}^- are of the similar order of magnitude above 200°C (this number is larger for hydrated electrons), Marin suggested that the diffusion rate of the hydrated electron is a factor of 3 times larger than extrapolated from lower temperatures at

300°C.[52] Therefore, the reason that reaction R5 is faster than R3 at these temperatures is likely due to a faster diffusion rate of the hydrated electron rather than a larger reaction distance.

Comparison of different Hydrogen abstraction reactions

The rate constants of Reaction R2 and R10 drop significantly at high temperatures due to Coulomb interaction, thus, they should be insignificant in SCWRs. R5 is diffusion-controlled below the critical point. However, orientation is an important factor for this reaction, thus it is heavily influenced by the cage effect and the reaction becomes activation controlled above the critical point. R16, R19 and R20 are all activation-controlled reactions that are influenced by the cage effect, their rate constants decrease near the critical point similar to R4. The shape of this type of temperature dependency is discussed in section 2.2.

2.4 Addition dissociation / Dissociative attachment

All reactions in this category involved two processes -addition and dissociation. The reactions in this section are less important than Reaction R3, R4, R5, R6 and R7 due to the small g-values of some reactants, thus they are discussed in the SI. At low temperatures, some reactions are activation-controlled and some reactions are diffusion-controlled. Above the critical point, all the addition dissociation/dissociative attachment reactions are activation-controlled due to the cage effect. This type of temperature dependency is discussed in detail in section 2.2.

2.5 Dissociation

There is only one reaction in this category. The g-value of the reactant, H_2O_2, is expected to be lower than those of ·OH, e_{aq}^-, H· and H_2 in SCW as described in section 2.6, thus this reaction is discussed in the SI.

2.6 General discussion of the temperature dependence

Here we include both equilibrium and non-equilibrium reactions. The most important reactions are those that involve water molecules because there is a high concentration of water. These reactions can be particularly important at high temperatures; for example, R32r becomes the main channel for ·OH and H_2 formation at elevated temperatures. Transient species that we need to pay attention to are e_{aq}^-, H_2, H· and ·OH, as experimental data suggests they are the major radiolysis species produced at around 350 °C.[8] We find that the reactions, R30f, R23r and other reactions that involve opposite charged reactants have the highest rate constants above the critical point. The rate constants for the reactions studied in this series over the temperature range of 20 to 900°C at a pressure of 250 bar are plotted in Figure 10 andFigure 11.

Note that the lower rate constants doesn't mean these reactions are not important; e.g. R32r is one of the most important reactions in supercritical water radiolysis.[56,57,61] The reactions that involve oppositely charged reactants need more attention, as our prediction shows the rate constants for this type of reactions increase dramatically at high temperatures.[7] An example of this type of reaction is R30f. R30f needs special attention because it might be the cause of the increase of H· atom yield in SCW compared to vapor. The significant increase of the rate constants for these reaction types is caused by the attractive force between the reactants in a low dielectric constant medium. The reverse reactions of these are slowed down very significantly in SCW.[7] For reactions that involve charged reactants, a further modification, including the effect of the dielectric constant, was also needed. This was done by adding a Debye correction factor.

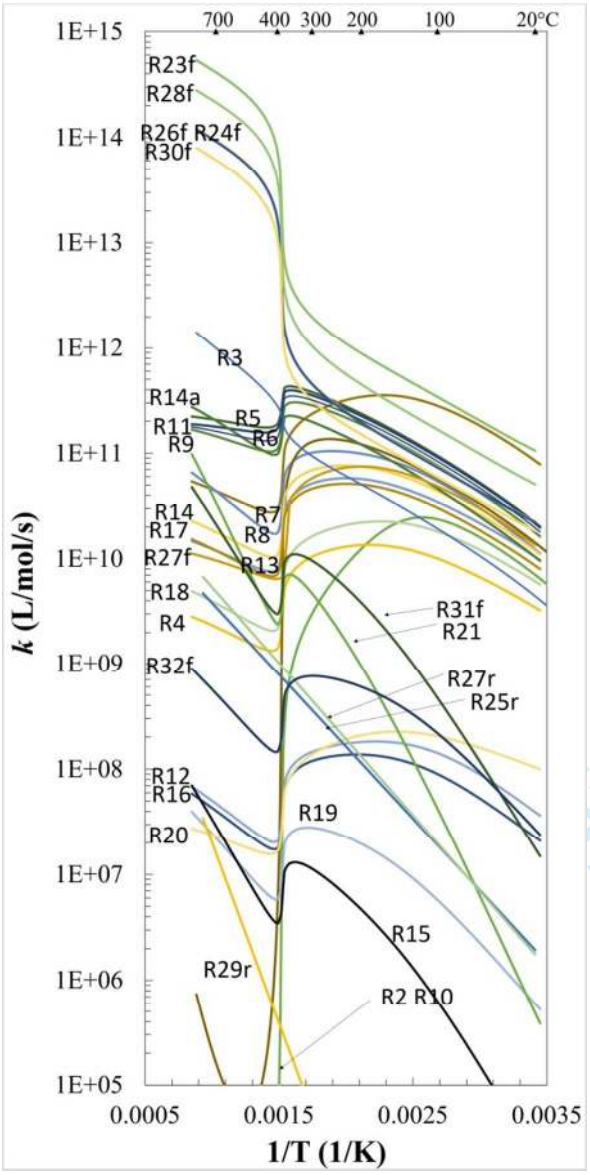

446

447 Figure 10 The plot of k_{pre} for all the reactions that were studied in this series with a
448 temperature range of 20 to 900°C at a pressure of 250 bar (the reactions with lower rate
449 constants are shown in Figure 11.

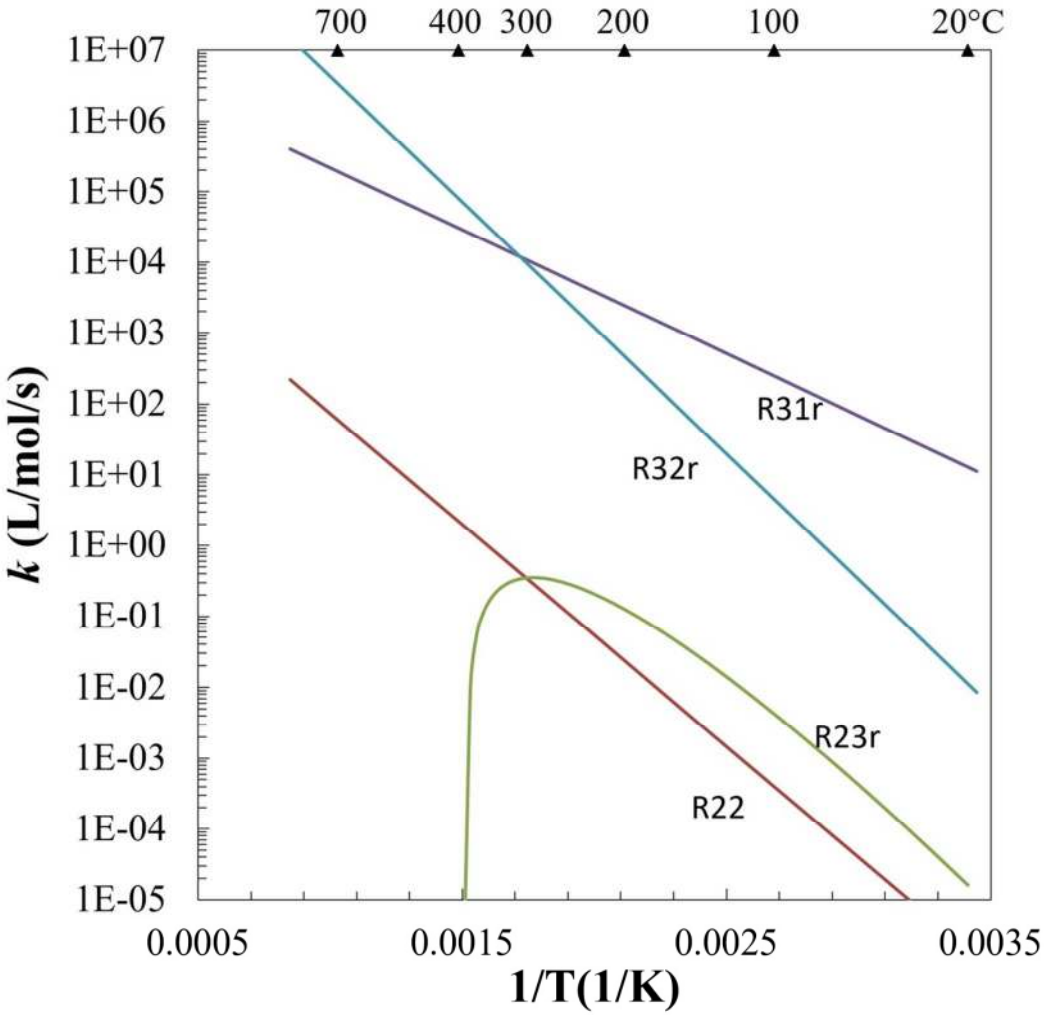

Figure 11 The rate constants for reactions that have lower rate constants than the reactions in Figure 10. Reactions like R23r (and R24r, R26r, R28r) are insignificant in supercritical water due to the decreases of the dielectric constant, which describe how well a medium supports ions. The rate constants of R23r are shown in the figure as an example; others are not shown.

The rate constants of R2 decrease significantly above 150°C. This sudden drop in rate constants reduces the formation of H_2 through this channel. R32r, on the other hand, becomes the significant channel for H_2 formation at high temperature. The H_2 formed through R32r will balance the effect of a decreasing rate constant of R2, so we predict that the g-value of H_2 will

459 continuously increase.[56,62] We expect the yield of H_2 to further increase at higher SCWR
460 temperatures. Bartels *et al.* proposed that the spur recombination reactions that produce H_2 are
461 mainly through the channel of R2, R3, and R5.[63] They conclude that the g-value of H_2 is mainly
462 caused by a pre-solvation event rather than spur recombination events using NO_3^- and $Cr_2O_7^{2-}$
463 as a hydrated electron scavengers, completely ignoring the effect of R32r.[63] They cited an
464 unpublished manuscript which suggests the g-value of H_2 remains unchanged with H· atom
465 scavenger phenol, which suggests the reaction R32r is not the cause of the increasing g-value
466 of H_2 at high temperature.[63] We, however, could not find this source, and we are not convinced
467 R32r is not important at high temperatures.

468 In a recent study by Katsumura's group,[64] the concentration of O_2 produced in their simulation
469 was increased by a factor of 100 if they used a rate constant for R32r of more than 10^3 M^{-1} s^{-1}
470 rather than neglecting the rate constant of R32r.[64] They suggested that the ·OH radicals
471 produced from R32r can react via R16 to produce HO_2, which is the source of O_2 production.[64]
472 Thus, R32r is a very important reaction for determining the yield of O_2 in water radiolysis. We
473 have experimentally determined the rate constant of R32r to be around 10^4 M^{-1} s^{-1} at 400°C
474 using the muon method.[19] In a recent pulse radiolysis study by Muroya *et al.*,[58] R32r was
475 studied by using I as a scavenger for OH·, by which an absorption spectrum of the produced I_2^-
476 was gathered. At 350°C, they found a rate constant for this reaction to be slightly larger than but
477 consistent with what we predicted.[58] These experiential result show that R32r is a very important
478 reaction in water radiolysis at high temperatures. We have developed a muon spin resonance
479 setup that can further increase the limit of our study to at least 550°C at 250 bar.[17] Experimental
480 data on R32r in this temperature and pressure range will be available soon.

The H_2O_2 is mainly formed through the channel R4 at lower temperatures.[61] Due to the cage effect, the rate constants for R4 will be lower above the critical point. As such we predict that the g-value of H_2O_2 should be low above the critical point.

At high temperatures, the rate constants of the main reactions that consume ·OH, namely R4, R6, R7, and R27f, are decreased. However, the reverse reaction of R32r becomes a significant channel that produces ·OH radical and H_2, so it is likely that the concentration of ·OH will be continuously increasing in SCW as temperature increases. Concerning H_2 production, less is formed through the channel of the R3 and R5 as a result of the cage effect. Above the critical point, we expect R30f to be very significant, which will turn H^+ and e_{aq}^- to H· (R30f is likely the cause of the decrease in g-value of e_{aq}^- at around 300°C[8]), this together with R32f will very likely to increase the g-value of H_2 and ·OH radical in SCW dramatically. On the other hand, since the dielectric constant, which describes how well a solvent can support ions, decreases with temperature in water, we expect the g-value for e_{aq}^- to continue decreasing above the critical point. However, e_{aq}^- is still a very important radiolysis species that should be studied very carefully, since it is initially largely produced in the spur (~10^{-12}s), and then are consumed through other reactions (from ~10^{-12}s to ~10^{-6}s).[6] The decrease in its g-value is likely due to being largely consumed through the channel of R30f. R7 is an important reaction. The yields for both of the reactants increase as the temperature increases to the critical point.[8] Both reactants could be produced a lot in SCW radiolysis. The two data sets we used to fit R7 are parallel, but one has consistently higher rate constants than the other. Re-measurement is recommended using the up-to-date extinction coefficients.

The reactions that did not have any existing data are R11, R15, R24f, R26f, R25f, and R29f. The reactions that have single data points are R10, R27, and R28. Among these reactions, R24f,

R26f, and R28f involve oppositely charged reactants. Those three reactions are expected to be very fast at high-temperatures, and they should be treated with special attention. More theoretical studies on reactions that involve oppositely charged reactants need to be done in order to better understand the radiolysis of water. This can be done based on knowledge of these types of reactions in other solvents. Our group is doing more studies on these types of reactions. Additional correction to critical fluctuation is needed in order to more accurately model the behavior of the reactions at conditions close to maximum compressibility.[19, 67, 68, 72] Also, influences of pH on rate constants for each reaction need to be considered. For example, SCWRs will operate in nearly-neutral water, and nearly-neutral water would more readily go through R20 than R19. It is therefore particularly important to make sure the rate constants apply to nearly-neutral water in future work. The recommended rate constants for non-equilibrium reactions R2 to R22a in a temperature range of 400 to 800°C with a pressure of 250 bar are provided in table format (Tables S3 and S4) in the SI.

2.7 General discussion of the pressure dependence

Most of the experimental data are at a low-temperature range, below 300°C. The pressures used in each individual experiment varied and were usually significantly lower than the pressure needed for SCWR. The first question is on the validity of such experimental data and models based on them for higher pressures. Pressure does not have a significant effect on rate constants at low temperatures. This is demonstrated in Figure 12 which shows the reproduced rate constants of fitted R17 at different pressures.

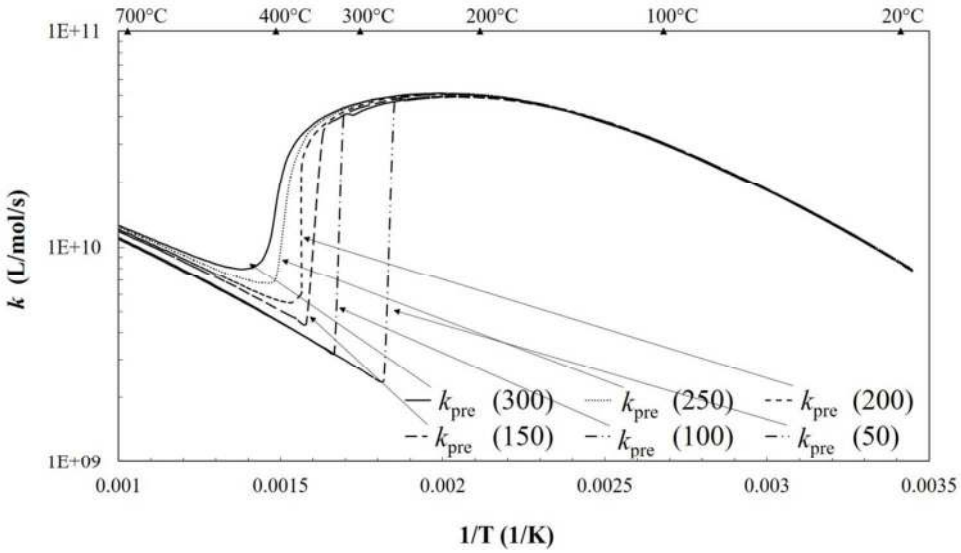

524 Figure 12 The rate constants of R17 at different pressures. Notice that although the rate
525 constants are significantly different at high-temperature ranges at different pressures, the rate
526 constants do not vary much with pressure at low temperatures.

527 Notice that although pressure has significant effects on rate constants at high temperatures,
528 the rate constants overlap at low temperatures. This show that pressure has very little influence
529 on rate constants below 300°C. Unless there is a phase change where the pressure is not
530 sufficient for water to maintain its liquid form, the rate constants are practically pressure
531 independent at low temperatures under 300°C. This is important because many experimental
532 works do not report the pressure used. Based on Figure 12, the data from low-temperatures can
533 be used regardless of pressure. Also, as shown in our previous work,[7] although Yoshida's
534 diffusion coefficient experimental data is taken from different pressures, all data points at a low-
535 temperature range (below 300°C) fit the Kallikragas and Stoke-Einstein models for diffusion
536 well. It is, therefore, valid for us to use the rate constants from experiments at low temperatures
537 and pressures to predict the rate constants above the critical point, as long as our model takes
538 into account the effects of the pressure at high temperatures, which it does. The effect of
539 pressure on reaction rate can be inferred from activation volume which is defined as the

difference between the partial molar volumes of the activated complex and the reactants.[65] From transition state theory, and classical thermodynamics, the pressure-dependent activation volume can be written as:

$$\left(\frac{\partial Ln(k)}{\partial P}\right)_T = -\frac{\Delta V^{\ddagger}}{RT} + \kappa_T$$

where *P* is the pressure, *R* is the gas constant, *T* is the temperature, k is rate constant, and κ_T is the solvent's isothermal compressibility.[66]

Properties such as density, diffusivity of water, compressibility and dielectric constant of the liquid can change significantly with pressure near the critical point. The change of those properties influence reaction kinetics.[11,65,67] However, away from the critical point, liquid properties are essentially pressure independent.[65] Based on our studies,[11] at 205°C, the isothermal rate constants of Mu· reacting with Ni^{2+} in water are essentially pressure independent. However, at 359°C, we observe a significant pressure dependence.[11] Similar behavior has been seen for the reaction between Mu· and hydroquinone in water.[11] From these previous works we established that activation volumes are only large enough at above 350°C.

3. Conclusion

Many properties of water depend on temperature and density, and this can significantly change the rate constants of reactions.[10,11,13,15,67–80] These include the efficiency factor (cage effect),[7] the diffusion rate of different species, and the dielectric constant that influences the reactions of charged species. In this work, we considered all these aspects. The main purpose of this study was to provide recommendations for rate constants of reactions in water past the critical point. We studied important reactions involved in the radiolysis of water using the "cage effect model".[7]

The cage effect model describes the drastic non-Arrhenius temperature dependence observed for different chemical reactions in water. The rate constants of many reactions follow Arrhenius temperature dependence at low temperatures. However, due to the cage effect, the reaction efficiency decreases at high temperatures. As a result, the rate constants of these reactions also decrease near the critical point. There is one collision per encounter for chemical reactions at high temperatures in SCW, thus the reaction efficiency remains constant in this high temperature range. Therefore, the rate constants of these reactions increase again and follow an Arrhenius temperature dependence at high temperatures. Our work will enable engineers to better predict the concentration of eroding species in SCWRs and allow them to develop chemical control strategies to minimize corrosion, thus increase the lifetime of the reactors.[17]

4. Acknowledgements

We thank Logan Toth, Rejean Leblanc, Tait Du and John Beninger for early help related to the development of some of our reaction models and Dr. Percival for valuable discussions. This research was financially supported by the Generation IV Energy Technologies Program of the Natural Sciences and Engineering Research Council of Canada and NSERC.

5. References:

(1) Yetisir, M.; Diamond, W.; Leung, L. K. H.; Martin, D.; Duffey, R. In *proceedings of the 5th International Symposium of the Supercritical Water Reactors (ISSCWR-5)*; Vancouver, **2011**.

(2) Generation IV International Forum. *A Technology Roadmap for Generation IV Nuclear Energy Systems*; Report GIF-002-00, **2002**.

(3) Kim, T. K. In *Nuclear Energy: Selected Entries from the Encyclopedia of Sustainability Science and Technology*; Tsoulfanidis, N., Ed.; Springer New York: New York, NY, **2013**; pp 175–201.

(4) Uchida, S.; Katsumura, Y. *J. Nucl. Sci. Technol.* **2013**, *50* (4), 346–362 DOI: 10.1080/00223131.2013.773171.

(5) Cobut, V.; Frongillo, Y.; Patau, J. P.; Goulet, T.; Fraser, M. J.; Jay-Gerin, J. P. *Radiat. Phys. Chem.* **1998**, *51* (3), 229–243 DOI: 10.1016/S0969-806X(97)00096-0.

(6) Frongillo, Y.; Goulet, T.; Fraser, M.-J.; Cobut, V.; Patau, J. P.; Jay-Gerin, J.-P. *Radiat. Phys. Chem.* **1998**, *51* (3), 245–254 DOI: 10.1016/S0969-806X(97)00097-2.

(7) Liu, G.; Du, T.; Toth, L.; Beninger, J.; Ghandi, K. *CNL Nucl. Rev.* **2016** DOI: 10.12943/CNR.2016.00035.

(8) A. J. Elliot and D. M. Bartels. *The Reaction Set, Rate Constants and G-Values for the Simulation of the Radiolysis of Light Water over the Range 20 to 350 °C Based on Information Available in 2008*; Atomic Energy of Canada Limited, Report,153-127160-450-001, **2009**.

(9) Brodovitch, J.-C.; McCollum, B. M.; Percival, P. W. *Phys. B Condens. Matter* **2009**, *404* (5–7), 950–952 DOI: 10.1016/j.physb.2008.11.129.

(10) Cline, J.; Takahashi, K.; Marin, T. W.; Jonah, C. D.; Bartels, D. M. *J. Phys. Chem. A* **2002**, *106* (51), 12260–12269 DOI: 10.1021/jp0270250.

(11) Ghandi, K.; Addison-Jones, B.; Brodovitch, J.-C.; McKenzie, I.; Percival, P. W.; Schüth, J. *Phys. Chem. Chem. Phys.* **2002**, *4* (4), 586–595 DOI: 10.1039/b108656a.

(12) Janik, I.; Bartels, D. M.; Marin, T. W.; Jonah, C. D. *J. Phys. Chem. A* **2007**, *111* (1), 79–88 DOI: 10.1021/jp065140v.

(13) Percival, P. W.; Brodovitch, J.-C.; Ghandi, K.; McCollum, B. M.; McKenzie, I. *Radiat. Phys. Chem.* **2007**, *76* (8–9), 1231–1235 DOI: 10.1016/j.radphyschem.2007.02.010.

(14) Ghandi, K.; Addison-Jones, B.; Brodovitch, J. C.; Kecman, S.; McKenzie, I.; Percival, P. W. *Phys. B Condens. Matter* **2003**, *326* (1–4), 55–60 DOI: 10.1016/S0921-4526(02)01572-7.

(15) Ghandi, K.; Percival, P. W. *J. Phys. Chem. A* **2003**, *107* (17), 3005–3008 DOI: 10.1021/jp027858q.

(16) Lin, M.; Muroya, Y.; Baldacchino, G.; Katsumura, Y. In *Recent trend in radiation chemistry*; Wishart JF, BSM, R., Eds.; World Scientific Publishing: Singapore, **2010**; pp 255–277.

(17) Liu, G.; Chen, Y.; Morrison, A.; Percival, P.; Ghandi, K. In *μSR2017 conference proceeding*; **2017**.

(18) Dougherty, R. C. *J. Chem. Phys.* **1998**, *109* (17), 7372–7378 DOI: 10.1063/1.477343.

(19) Alcorn, C. D.; Brodovitch, J. C.; Percival, P. W.; Smith, M.; Ghandi, K. *Chem. Phys.* **2014**, *435*, 29–39 DOI: 10.1016/j.chemphys.2014.02.016.

(20) Janik, I.; Bartels, D. M.; Jonah, C. D. *J. Phys. Chem. A* **2007**, *111* (10), 1835–1843 DOI: 10.1021/jp065992v.

(21) Elliot, A. J.; McCracken, D. R.; Buxton, G. V.; Wood, N. D. *J. Chem. Soc. Faraday Trans.* **1990**, *86* (9), 1539 DOI: 10.1039/ft9908601539.

(22) Zheng, J.; Fayer, M. D. *J. Am. Chem. Soc.* **2007**, *129* (14), 4328–4335 DOI: 10.1021/ja067760f.

(23) Mizan, T. I.; Savage, P. E.; Ziff, R. M. *J. Phys. Chem.* **1996**, *100* (1), 403–408 DOI: 10.1021/jp951561t.

(24) Sehested, K.; Christensen, H. *Int. J. Radiat. Appl. Instrumentation. Part C. Radiat. Phys. Chem.* **1990**, *36* (3), 499–500 DOI: 10.1016/1359-0197(90)90040-O.

(25) Senba, M. *Phys. Rev. A* **1994**, *50* (1), 214–227 DOI: 10.1103/PhysRevA.50.214.

(26) Kallikragas, D. T.; Plugatyr, A. Y.; Svishchev, I. M. *J. Chem. Eng. Data* **2014**, *59* (6), 1964–1969 DOI: 10.1021/je500096r.

(27) Svishchev, I. M.; Carvajal-Ortiz, R. A.; Choudhry, K. I.; Guzonas, D. A. *Corros. Sci.* **2013**, *72*, 20–25 DOI: 10.1016/j.corsci.2013.02.005.

(28) Kanike, V.; Meesungnoen, J.; Jay-Gerin, J.-P. *RSC Adv.* **2015**, *5* (54), 43361–43370 DOI: 10.1039/C5RA07173A.

(29) Christensen, H.; Sehested, K.; Logager, T. *Radiat. Phys. Chem.* **1994**, *43* (6), 527–531 DOI: 10.1016/0969-806X(94)90163-5.

(30) Elliot, A. J.; Ouellette, D. C. *J. Chem. Soc., Faraday Trans.* **1994**, *90* (6), 837–841 DOI: 10.1039/FT9949000837.

(31) Lundström, T.; Christensen, H.; Sehested, K. *Radiat. Phys. Chem.* **2002**, *64* (1), 29–33 DOI: 10.1016/S0969-806X(01)00439-X.

(32) Buxton, G. V.; Elliot, A. J. *J. Chem. Soc. Faraday Trans.* **1993**, *89* (3), 485 DOI: 10.1039/ft9938900485.

(33) Swiatla-Wojcik, D.; Buxton, G. V. *J. Phys. Chem.* **1995**, *99* (29), 11464–11471 DOI: 10.1021/j100029a026.

(34) Gaussian 09, Revision A.02, M. J. Frisch, G. W. Trucks, H. B. Schlegel, G. E. Scuseria, M. A. Robb, J. R. Cheeseman, G. Scalmani, V. Barone, G. A. Petersson, H. Nakatsuji, X. Li, M. Caricato, A. Marenich, J. Bloino, B. G. Janesko, R. Gomperts, B. Mennucci, H. P. Hratchian, J. V. Ortiz, A. F. Izmaylov, J. L. Sonnenberg, D. Williams-Young, F. Ding, F.

650 Lipparini, F. Egidi, J. Goings, B. Peng, A. Petrone, T. Henderson, D. Ranasinghe, V. G.
651 Zakrzewski, J. Gao, N. Rega, G. Zheng, W. Liang, M. Hada, M. Ehara, K. Toyota, R.
652 Fukuda, J. Hasegawa, M. Ishida, T. Nakajima, Y. Honda, O. Kitao, H. Nakai, T. Vreven, K.
653 Throssell, J. A. Montgomery, Jr., J. E. Peralta, F. Ogliaro, M. Bearpark, J. J. Heyd, E.
654 Brothers, K. N. Kudin, V. N. Staroverov, T. Keith, R. Kobayashi, J. Normand, K.
655 Raghavachari, A. Rendell, J. C. Burant, S. S. Iyengar, J. Tomasi, M. Cossi, J. M. Millam,
656 M. Klene, C. Adamo, R. Cammi, J. W. Ochterski, R. L. Martin, K. Morokuma, O. Farkas, J.
657 B. Foresman, and D. J. Fox, Gaussian, Inc., Wallingford CT, **2016**.

658 (35) R.G.Parr; W.Yang. *Density Functional Theory of Atoms and Molecules*; Oxford University
659 Press: Oxford, UK, **1989**.

660 (36) Becke, A. D. *J. Chem. Phys.* **1993**, *98* (7), 5648–5652 DOI: 10.1063/1.464913.

661 (37) Lee, C.; Yang, W.; Parr, R. G. *Phys. Rev. B* **1988**, *37* (2), 785–789 DOI:
662 10.1103/PhysRevB.37.785.

663 (38) Krishnan, R.; Binkley, J. S.; Seeger, R.; Pople, J. A. *J. Chem. Phys.* **1980**, *72* (1), 650–
664 654 DOI: 10.1063/1.438955.

665 (39) Peng, C.; Bernhard Schlegel, H. *Isr. J. Chem.* **1993**, *33* (4), 449–454 DOI:
666 10.1002/ijch.199300051.

667 (40) Fernández-Ramos, A.; Miller, J. A.; Klippenstein, S. J.; Truhlar, D. G. *Chem. Rev.* **2006**,
668 *106* (11), 4518–4584 DOI: 10.1021/cr050205w.

669 (41) Lynch, B. J.; Truhlar, D. G. *J. Phys. Chem. A* **2001**, *105* (13), 2936–2941 DOI:
670 10.1021/jp004262z.

671 (42) Marsalek, O.; Uhlig, F.; VandeVondele, J.; Jungwirth, P. *Acc. Chem. Res.* **2012**, *45* (1),
672 23–32 DOI: 10.1021/ar200062m.

673 (43) Garrett, B. C.; Dixon, D. A.; Camaioni, D. M.; Chipman, D. M.; Johnson, M. A.; Jonah, C.
674 D.; Kimmel, G. A.; Miller, J. H.; Rescigno, T. N.; Rossky, P. J.; Xantheas, S. S.; Colson, S.
675 D.; Laufer, A. H.; Ray, D.; Barbara, P. F.; Bartels, D. M.; Becker, K. H.; Bowen, K. H.;
676 Bradforth, S. E.; Carmichael, I.; Coe, J. V.; Corrales, L. R.; Cowin, J. P.; Dupuis, M.;
677 Eisenthal, K. B.; Franz, J. A.; Gutowski, M. S.; Jordan, K. D.; Kay, B. D.; LaVerne, J. A.;
678 Lymar, S. V.; Madey, T. E.; McCurdy, C. W.; Meisel, D.; Mukamel, S.; Nilsson, A. R.;
679 Orlando, T. M.; Petrik, N. G.; Pimblott, S. M.; Rustad, J. R.; Schenter, G. K.; Singer, S. J.;
680 Tokmakoff, A.; Wang, L.-S.; Zwier, T. S. *Chem. Rev.* **2005**, *105* (1), 355–390 DOI:
681 10.1021/cr030453x.

682 (44) von Sonntag, C. *Free-Radical-Induced DNA Damage and Its Repair*; Springer Berlin
683 Heidelberg: Berlin, Heidelberg, **2006**.

684 (45) Alizadeh, E.; Sanche, L. *Chem. Rev.* **2012**, *112* (11), 5578–5602 DOI: 10.1021/cr300063r.

685 (46) Abel, B.; Buck, U.; Sobolewski, a L.; Domcke, W. *Phys. Chem. Chem. Phys.* **2012**, *14* (1),

22–34 DOI: 10.1039/c1cp21803d.

(47) Herbert, J. M.; Jacobson, L. D. *Int. Rev. Phys. Chem.* **2011**, *30* (1), 1–48 DOI: 10.1080/0144235X.2010.535342.

(48) Turi, L.; Rossky, P. J. *Chem. Rev.* **2012**, *112* (11), 5641–5674 DOI: 10.1021/cr300144z.

(49) Abel, B. *Annu. Rev. Phys. Chem.* **2013**, *64* (1), 533–552 DOI: 10.1146/annurev-physchem-040412-110038.

(50) Herbert, J. M.; Coons, M. P. *Annu. Rev. Phys. Chem.* **2017**, *68* (1), 447–472 DOI: 10.1146/annurev-physchem-052516-050816.

(51) Christensen, H.; Sehested, K. *J. Phys. Chem.* **1986**, *90* (1), 186–190 DOI: 10.1021/j100273a042.

(52) Marin, T. W.; Takahashi, K.; Jonah, C. D.; Chemerisov, S. D.; Bartels, D. M. *J. Phys. Chem. A* **2007**, *111* (45), 11540–11551 DOI: 10.1021/jp074581r.

(53) Elliot, A.; Ouellette, D. C.; Stuart, C. R. *The Temperature Dependence of the Rate Constants and Yields for the Simulation of the Radiolysis of Heavy Water*; Atomic Energy of Canada Limited, Report: AECL-11658, **1996**.

(54) Barnett, R. N.; Giniger, R.; Cheshnovsky, O.; Landman, U. *J. Phys. Chem. A* **2011**, *115* (25), 7378–7391 DOI: 10.1021/jp201560n.

(55) Butarbutar, S. L.; Muroya, Y.; Kohan, L. M.; Sanguanmith, S.; Meesungnoen, J.; Jay-Gerin, J.-P. *Atom Indones.* **2013**, *39* (2), 51 DOI: 10.17146/aij.2013.231.

(56) Sanguanmith, S.; Muroya, Y.; Meesungnoen, J.; Lin, M.; Katsumura, Y.; Mirsaleh Kohan, L.; Guzonas, D. a.; Stuart, C. R.; Jay-Gerin, J.-P. *Chem. Phys. Lett.* **2011**, *508* (4–6), 224–230 DOI: 10.1016/j.cplett.2011.04.059.

(57) Swiatla-Wojcik, D.; Buxton, G. V. *Radiat. Phys. Chem.* **2005**, *74* (3–4), 210–219 DOI: 10.1016/j.radphyschem.2005.04.014.

(58) Muroya, Y.; Yamashita, S.; Lertnaisat, P.; Sanguanmith, S.; Meesungnoen, J. *Phys. Chem. Chem. Phys.* **2017**, *19* (45), 30834–30841 DOI: 10.1039/C7CP06010F.

(59) Schwarz, H. A. *J. Phys. Chem.* **1992**, *96* (22), 8937–8941 DOI: 10.1021/j100201a044.

(60) Hare, P. M.; Price, E. a; Bartels, D. M. *J. Phys. Chem. A* **2008**, *112* (30), 6800–6802 DOI: 10.1021/jp804684w.

(61) Sanguanmith, S.; Meesungnoen, J.; Jay-Gerin, J.-P. *Chem. Phys. Lett.* **2013**, *588*, 82–86 DOI: 10.1016/j.cplett.2013.09.057.

(62) Sterniczuk, M.; Yakabuskie, P. A.; Wren, J. C.; Jacob, J. A.; Bartels, D. M. *Radiat. Phys.*

Chem. **2016**, *121*, 35–42 DOI: 10.1016/j.radphyschem.2015.12.007.

(63) Sterniczuk, M.; Bartels, D. M. *J. Phys. Chem. A* **2016**, *120* (2), 200–209 DOI: 10.1021/acs.jpca.5b12281.

(64) Lertnaisat, P.; Katsumura, Y.; Mukai, S.; Umehara, R.; Shimizu, Y.; Suzuki, M. *J. Nucl. Sci. Technol.* **2016**, *53* (11), 1816–1823 DOI: 10.1080/00223131.2016.1165636.

(65) Wu, B. C.; Klein, M. T.; Sandler, S. I. *Ind. Eng. Chem. Res.* **1991**, *30* (5), 822–828 DOI: 10.1021/ie00053a003.

(66) Savage, P. E.; Gopalan, S.; Mizan, T. I.; Martino, C. J.; Brock, E. E. *AIChE J.* **1995**, *41* (7), 1723–1778 DOI: 10.1002/aic.690410712.

(67) Ghandi, K.; McFadden, R. M. L.; Cormier, P. J.; Satija, P.; Smith, M. *Phys. Chem. Chem. Phys.* **2012**, *14* (24), 8502 DOI: 10.1039/c2cp41170a.

(68) Cormier, P. J.; Clarke, R. M.; McFadden, R. M. L.; Ghandi, K. *J. Am. Chem. Soc.* **2014**, *136* (6), 2200–2203 DOI: 10.1021/ja408438s.

(69) Satija, P.; McFadden, R. M. L.; Cormier, P.; Ghandi, K. *Int. Rev. Chem. Eng.* **2011**, *3* (5), 542–549.

(70) Cormier, P.; Arseneau, D. J.; Brodovitch, J. C.; Lauzon, J. M.; Taylor, B. A.; Ghandi, K. *J. Phys. Chem. A* **2008**, *112* (20), 4593–4600 DOI: 10.1021/jp801023v.

(71) Ghandi, K.; Brodovitch, J.-C.; Addison-Jones, B.; Percival, P. W.; Schüth, J. *Phys. B Condens. Matter* **2000**, *289–290*, 476–481 DOI: 10.1016/S0921-4526(00)00440-3.

(72) Cormier, P. J.; Alcorn, C.; Legate, G.; Ghandi, K. *Radiat. Res.* **2014**, *181* (4), 396–406 DOI: 10.1667/RR13516.1.

(73) Legate, G.; Alcorn, C.; Brodovitch, J.-C.; Ghandi, K.; Percival, P. W. In *proceedings of the 5th International Symposium of the Supercritical Water Reactors (ISSCWR-5)*; **2011**.

(74) Ghandi, K.; Alcorn, C.; Legate, G.; Percival, P. W.; Brodovitch, J.-C. In *proceedings of the second Canada-China Joint Conference on Supercritical Water-Cooled Reactors*; **2010**.

(75) Lin, M.; Katsumura, Y.; Muroya, Y.; He, H.; Wu, G.; Han, Z.; Miyazaki, T.; Kudo, H. *J. Phys. Chem. A* **2004**, *108* (40), 8287–8295 DOI: 10.1021/jp048854j.

(76) Muroya, Y.; Lin, M.; de Waele, V.; Hatano, Y.; Katsumura, Y.; Mostafavi, M. *J. Phys. Chem. Lett.* **2010**, *1* (1), 331–335 DOI: 10.1021/jz900225a.

(77) Bartels, D. M.; Takahashi, K.; Cline, J. A.; Marin, T. W.; Jonah, C. D. *J. Phys. Chem. A* **2005**, *109* (7), 1299–1307 DOI: 10.1021/jp0457141.

(78) Percival, P. W.; Brodovitch, J.-C.; Ghandi, K.; Addison-Jones, B.; Schüth, J.; Bartels, D.

M. *Phys. Chem. Chem. Phys.* **1999**, *1* (21), 4999–5004 DOI: 10.1039/a906925i.

(79) Bulemela, E.; Tremaine, P.; Ikawa, S. *Fluid Phase Equilib.* **2006**, *245* (2), 125–133 DOI: 10.1016/j.fluid.2006.05.007.

(80) Zimmerman, G. H.; Arcis, H.; Tremaine, P. R. *J. Chem. Eng. Data* **2012**, *57* (11), 3180–3197 DOI: 10.1021/je3007887.

Addition /Non dissociative attachment	
R3	$H\cdot + H\cdot \rightarrow H_2$
R4	$\cdot OH + \cdot OH \rightarrow H_2O_2$
R6	$e_{aq}^- + \cdot OH \rightarrow OH^-$
R7	$H\cdot + \cdot OH \rightarrow H_2O$
R9	$e_{aq}^- + O_2 \rightarrow O_2^-$
R11	$e_{aq}^- + HO_2 \rightarrow HO_2^-$
R13	$H\cdot + O_2 \rightarrow HO_2$
R14	$H\cdot + HO_2 \rightarrow H_2O_2$
R15	$H\cdot + O_2^- \rightarrow HO_2^-$
Hydrogen abstraction	
R2	$e_{aq}^- + e_{aq}^- + (2\ H_2O) \rightarrow H_2 + 2\ OH^-$
R5	$e_{aq}^- + H\cdot\ (+\ H_2O) \rightarrow H_2 + OH^-$
R10	$e_{aq}^- + O_2^-\ (+\ H_2O) \rightarrow H_2O_2 + 2\ OH^-$
R16	$\cdot OH + H_2O_2 \rightarrow HO_2 + H_2O$
R19	$HO_2 + HO_2 \rightarrow H_2O_2 + O_2$
R20	$O_2^- + HO_2 \rightarrow HO_2^- + O_2$
R21	$O_2^- + O_2^- + (H^+) \rightarrow HO_2^- + O_2$
Addition dissociation / Dissociative attachment	
R8	$e_{aq}^- + H_2O_2 \rightarrow \cdot OH + OH^-$
R12	$H\cdot + H_2O_2 \rightarrow \cdot OH + H_2O$
R14a	$H\cdot + HO_2 \rightarrow 2\ \cdot OH$
R17	$\cdot OH + O_2^- \rightarrow (HO_3^-) \rightarrow O_2 + OH^-$
R18	$\cdot OH + HO_2 \rightarrow (H_2O_3) \rightarrow O_2 + H_2O$
Dissociation	
R22	$H_2O_2 \rightarrow 1/2\ O_2 + H_2O$
R22a	$H_2O_2 \rightarrow 2\cdot OH$

Table 1 The reactions studied in this paper are classified according to their mechanisms.

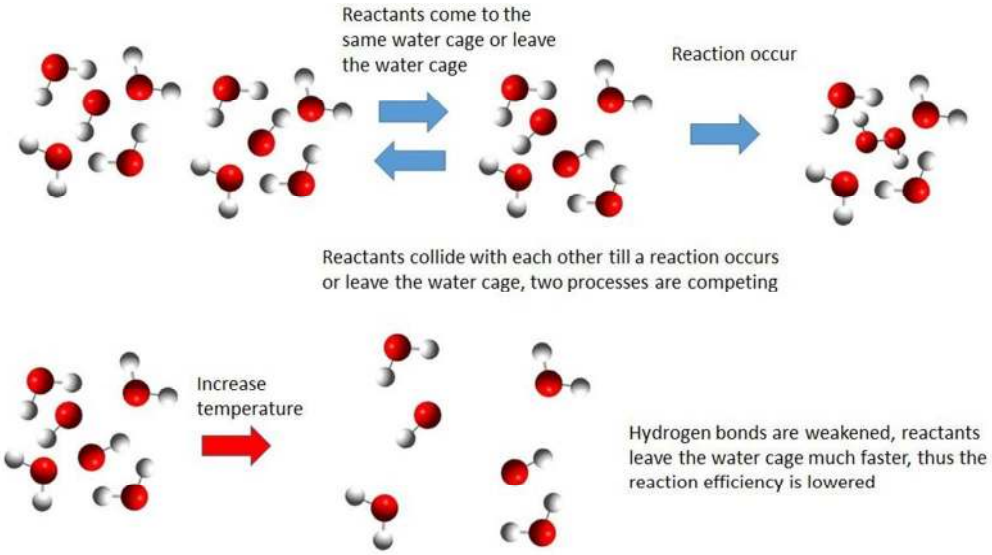

85x49mm (300 x 300 DPI)